

Uptake of gaseous formaldehyde by soil surfaces: a combination of adsorption/desorption equilibrium and chemical reactions

Guo Li^{1,2}, Hang Su¹, Xin Li³, Uwe Kuhn¹, Hannah Meusel¹, Thorsten Hoffmann⁴, Markus Ammann⁵,
5 Ulrich Pöschl¹, Min Shao^{2,*}, Yafang Cheng^{1,*}

¹Multiphase Chemistry Department, Max Planck Institute for Chemistry, Mainz, Germany

²College of Environmental Sciences and Engineering, Peking University, Beijing, China

³Institute for Energy and Climate Research, IEK-8, Research Center Jülich, Jülich, Germany

⁴Institute of Inorganic Chemistry and Analytical Chemistry, Johannes Gutenberg University Mainz, Mainz, Germany

10 ⁵Laboratory of Radiochemistry and Environmental Chemistry, Paul Scherrer Institute, 5232 Villigen, Switzerland

Correspondence to: Y. Cheng (yafang.cheng@mpic.de) or M. Shao (mshao@pku.edu.cn)

15

20

25

30

Abstract

Gaseous formaldehyde (HCHO) is an important precursor of OH radicals and a key intermediate molecule in the oxidation of atmospheric volatile organic compounds (VOCs). Budget analyses reveal large discrepancies between modeled and observed HCHO concentrations in the atmosphere. Here, we investigate the interactions of gaseous HCHO with soil surfaces through coated-wall flow tube experiments applying atmospherically relevant HCHO concentrations of ~10 to 40 ppbv. For the determination of uptake coefficients (γ), we provide a Matlab code to account for the diffusion correction under laminar flow conditions. Under dry conditions (relative humidity = 0%), an initial γ of $(1.1 \pm 0.05) \times 10^{-4}$ is determined, which gradually drops to $(5.5 \pm 0.4) \times 10^{-5}$ after 8-hour experiments. Experiments under wet conditions show a smaller γ that drops faster over time until reaching a plateau. The drop of γ with increasing relative humidity and over time can both be explained by the adsorption theory in which high surface coverage leads to a reduced uptake rate. The fact that γ stabilizes at a non-zero plateau suggests the involvement of irreversible chemical reactions. Further back-flushing experiments show that two thirds of the adsorbed HCHO can be re-emitted into the gas phase while the residual is retained by the soil. This partial reversibility confirms that HCHO uptake by soil is a complex process involving both adsorption/desorption and chemical reactions which must be considered in trace gas exchange (emission or deposition) at the atmosphere-soil interface. Our results suggest that soil and soil-derived airborne particles can either act as a source or a sink for HCHO, depending on ambient conditions and HCHO concentrations.

20

25

30

1 Introduction

Atmospheric HCHO represents one of the most abundant carbonyls in the atmosphere and is a key intermediate in atmospheric hydrocarbon oxidation. It is one of the major primary sources of HO_x (HO_x=HO+HO₂) radicals (Lowe and Schmidt, 1983;Fried et al., 1997;Hak et al., 2005;Seinfeld and Pandis, 2006) and it also serves as a large source in the global budget of H₂ and CO (Price et al., 2007). Around 90% of global tropospheric HCHO is produced by the oxidation of methane (CH₄) and non-methane volatile organic compounds (NMVOCs), while direct emissions from biomass burning and fossil fuel combustion contribute to the remaining fraction (Carrier et al., 1986;Lee et al., 1998;Andreae and Merlet, 2001;Parrish et al., 2012). The known removal processes of HCHO include reaction with OH radicals, photolysis, deposition and aerosol uptake, of which the first two pathways are supposed to dominate (Zhou et al., 1996;Tie et al., 2001;Fried et al., 2003).

Budget analyses, however, reveal large discrepancies between observed HCHO concentrations and those predicted from models (Jacob, 2000;Wagner et al., 2002). Overpredictions of HCHO have been reported in a series of studies since mid-1990s (Liu et al., 1992;Heikes et al., 1996;Jacob et al., 1996;Zhou et al., 1996). For example, a recent model study at a semi-rural site in southern China by Li et al. (2014) showed 2-5 times higher HCHO than observations. On the other hand, underpredictions have also been found in a few studies (Ayers et al., 1997;Jaegle et al., 2000;Weller et al., 2000;Kormann et al., 2003). The disagreement between model calculations and observations suggests an inadequate understanding of the HCHO budget and the existence of additional source/sink terms. For example, neglecting uptake of HCHO by aerosols/clouds (Zhou et al., 1996;Tie et al., 2001;Fried et al., 2003) may result in an overestimation while insufficient consideration of NMVOCs oxidation processes may lead to underestimated production of HCHO (Wagner et al., 2002). So far the imbalance in the HCHO budget remains inconclusive.

Soil and soil-derived mineral dust could represent an important kind of surfaces regulating the budget of several trace gases and aerosols in the atmosphere (Usher et al., 2003;Kulmala and Petaja, 2011;Su et al., 2011;Oswald et al., 2013;Donaldson et al., 2014a). Understanding the interactions of HCHO with soil surfaces may help to explain the discrepancies and improve our understanding of the HCHO budget. Some field flux measurements have found HCHO emission from soil surfaces (DiGangi et al., 2011) while other studies suggested a net HCHO deposition on soil surfaces (Gray et al., 2014).

In this study, we investigate the HCHO uptake on soil surfaces using a coated-wall flow tube method. The experiments are performed under conditions relevant to the atmosphere, i.e., HCHO concentrations of ~10 to 40 ppbv and relative humidities (RHs) of 0% to 70%. The uptake coefficients γ are determined by numerically solving the Cooney-Kim-Davis equation, which describes the loss of a trace species to the flow tube wall at laminar flow conditions (Murphy and Fahey, 1987). The results are discussed along with its underlying mechanisms and atmospheric implications.

2 Methods

2.1 Sample preparation

Soil samples were collected at a depth of 0-5 cm from a cultivated field site in Mainz, Germany (49°59'N, 8°13'E). The soil pH was ~7.5 (1:2 soil/water (v/v), Thermo Scientific, OrionStar A211 pH meter). The soil texture comprised 15% sand, 69% silt and 16% clay (wet sieving method) and the soil humus content was 3% (loss on ignition method) as analyzed by Envilytix GmbH (Wiesbaden, Germany). The collected samples were air-dried in the laboratory prior to grinding and sieving with a 120 mesh soil sieve. The sieved soil was autoclaved for 20 min at 394 K right before the flow tube coating procedure. Different soil types are inhabited by different microbial communities being very sensitive to soil properties (e.g., soil water content, pH, temperature, etc.). The applied wide range of changes in relative humidity within our experiments affects the soil water content, with respective impact on microbial activity. For a natural soil probe, the apportionment between the soil microbiological trace gas exchange and soil physicochemical effects would become vague, specifically in view of time-dependent patterns of microbial activity after changes in soil water content. The soil sterilization treatment eliminates the effects of microbiological activity on trace gas uptake/emission mechanism. The soil samples used in our study may serve as a soil proxy to study the physicochemical side of trace gas exchange, constituting a key element in regulating trace gas exchange at the atmosphere-soil interface (Donaldson et al., 2014b; VandenBoer et al., 2015). However, our results on sterilized soil samples cannot necessarily be considered representative for other and/or natural types of soils. The coating procedure is one of the challenges in flow tube experiments. Manually coating the tube could be time consuming and the coating thickness and homogeneity strongly depend on the operator. Here, an air-dried continuous rotating coating tool (ACRO) was developed to standardize the coating procedure and improve reproducibility and homogeneity (Fig.S.1). During the coating procedure, the tube was installed into the ACRO through two cylindrical fittings. One fitting was fixed to the inlet of the tube promoting tube rotation by means of a motor and a driving belt, while the other at the tube's outlet served only as a supporter not being fixed to the tube. The flow tube was normally placed horizontally but could also be tilted by adjusting the slope of ACRO (through a positioning screw). A drying air stream was piloted into the tube through a duct at the inlet connector.

25

Before coating, we prepared a soil slurry by mixing dry soil with sterilized deionized water obtained from a Milli-Q system (18.2 M Ω -cm, Millipore). The slurry was uniformly injected into an internally sandblasted glass tube which was then installed into the ACRO. The coated tube was rotated with a speed of 14 rpm and dried overnight with a flow rate of ~0.5 L min⁻¹ of pure N₂ (RH = 0%). The coating thickness/mass had been found to affect the trace gases uptake in earlier studies (Donaldson et al., 2014a). As the coating thickness increases, the uptake rate also increases due to enhanced number of surface sites available for gas uptake. Then the uptake rate moves up to a threshold level, where further increase in coating thickness doesn't affect the gas uptake. In order to exclude the influence of coating thickness, a relatively thick coating of ~500 μ m was chosen for our experiments. Figure 1 shows the homogeneous soil cover thickness and structural details of the

30

soil surface topography derived by scanning electron microscope (SEM). The good reproducibility of the experimental results as shown later also confirms the fair homogeneity and reproducibility of the coating.

2.2 Flow tube experiments

5 The uptake of HCHO onto soil surfaces was measured by employing a coated-wall flow tube system (see Fig. 2). The system consisted of four parts: (1) a HCHO generator; (2) a humidification unit; (3) a flow tube and reference tube unit; and (4) a detection unit. HCHO was generated from a solid permeation tube (formaldehyde-para, rate: 91 ng min^{-1} at $60 \text{ }^\circ\text{C}$, VICI Metronics Inc. U.S.A) with N_2 ($\geq 99.999\%$) as the carrier gas. The RH was controlled by mixing humidified N_2 with generated HCHO gas.

10 Two glass tubes (inner surface sandblasted) with identical dimensions (length: 250 mm, i.d.: 7 mm) were used for the uptake experiments. One tube was coated with soil samples and the other remained uncoated as a reference. Both tubes were placed in a cooling jacket in which a temperature of $296 \pm 1\text{K}$ was maintained during the experiments. HCHO concentrations were measured by an AL 4021 HCHO monitor (detection range: 100 ppt - 3 ppm, noise: 2% full scale, AERO LASER, Germany). It is an online HCHO analyzer for gaseous and liquid samples, based on the Hantzsch reaction. Gaseous HCHO is transferred into a liquid phase through a stripping coil, prior to reacting with Hantzsch reagents (ammonium acetate: for analysis, Merck, Germany; acetyl acetone: for analysis, Merck, Germany; and acetic acid (glacial): 100%, Merck, Germany).
15 The products show a strong fluorescence at 510 nm, which is measured by a photomultiplier. The operation principle is described in detail elsewhere (Dasgupta et al., 1988). This analyzer has been used for field measurements and has shown high stability (Preunkert et al., 2013; Preunkert et al., 2015). The flow rate used for our lab experiments was 1 L STP min^{-1} .
20 The analyzer was operated with liquid calibration gas measurement mode and was calibrated using standard HCHO solutions (37 wt% in H_2O , Sigma-Aldrich, U.S.A).

Several flow tube experiments were carried out to examine different aspects of the uptake processes, e.g., reproducibility, RH dependence, and bi-directional exchange, etc. In each experiment, we adopted the following procedure: (1) flushing the
25 freshly coated tube with pure N_2 ; (2) flushing the uncoated reference tube with HCHO; (3) flushing the freshly coated tube with HCHO. The first step was to detect background HCHO emission from soil. While the second step allowed for identification of potential uptake of HCHO on clean glass surface, the third step was dedicated to investigate HCHO uptake by the soil surface, from which uptake coefficients can be derived. To check the stability of the HCHO monitor and generator, we also performed zero calibrations for the monitor and measured the generated HCHO concentrations before and
30 after each experiment. As a wide range of RH conditions (0% - 70%) was applied in the uptake experiments, the potential effect of water molecules on the generated HCHO concentration and background (zero air) concentration was examined. At the outlet of the stripping coil, the sample air was saturated to 100% RH at 10°C . Depending on the inlet air RH (at room temperature) the stripping solution would gain (condensation) or lose (evaporation) water according to the gas/liquid phase

equilibrium (Junkermann and Burger, 2006). The bias in calculated HCHO concentrations was within $\pm 3\%$. To check the RH effect on measured HCHO concentration under varying RH conditions, we occasionally compared the observed concentrations with data derived from the certified permeation rate of the permeation tube and the measured gas flow rate (gas phase calibration method). The observed total bias, assumed to characterize the instrument's accuracy was within $\pm 5\%$.

5 Moreover, the instrument's zero air background was observed to increase gradually when increasing RH from 0% to 50%, and decreased when further increasing RH beyond 70%. This could be due to the RH effect on the measurement principle, inlet surface effects, or aging of peristaltic tubes, stripping solution and Hantzsch solution (Kaiser et al., 2014). To account for the influence of changed background on measured HCHO concentration, the background was checked at the beginning and end of each experiment and the measured HCHO concentrations were corrected based on observed background values.

10 On the other hand, well-known ozone interferences (Rodier and Birks, 1994; Kormann et al., 2003) were not of any concern for our studies, as the applied carrier gas was free of ozone.

2.3 Determination of uptake coefficients

The goal of our kinetic experiments is to determine the uptake coefficients γ . The parameter γ is defined as the fraction of effective collisions between HCHO and the soil surface that leads to loss of HCHO due to physical or chemical processes.

15 For investigations on trace gas uptake kinetics using flow tubes, a method, designated the CKD solution (Murphy and Fahey, 1987), is commonly applied to account for radial and axial diffusion effects. Here we develop a new method rather than using the interpolated values provided in CKD method. As our method is based on the CKD, it can be specified as CKD-based method (CKD-B). For the details of CKD-B, see Appendix A. In our experiment, the Reynolds number R_e is ~ 200 ensuring the laminar flow conditions which require $R_e < \sim 2100$ (Murphy and Fahey, 1987). The total flow tube length is 25

20 cm and full development of laminar flow is achieved within ~ 5 cm for our setup. The uptake coefficients reported here are based on the geometric surface area of the soil sample, considering that in atmospheric models soil microstructure is not taken into account. In order to facilitate modelling, the calculated uptake coefficients as a function of initial HCHO concentration, relative humidity and uptake time period are summarized in Table S.1. The specific surface area of the soil sample, however, was also measured using a water vapor adsorption method based on the Brunauer-Emmett-Teller (BET)

25 adsorption theory (Brunauer et al., 1938) being $18.9 \pm 1.3 \text{ m}^2 \text{ g}^{-1}$. For calculating this BET surface area, the mass of the adsorbed water on soil sample after equilibrium with pre-defined RH levels was determined by a non-dispersive infrared (NDIR) gas analyzer (type: Li-6262, LI-COR Biosciences Inc.) operated in differential mode. This BET surface area is comparable to that in other reports on similar soil types, e.g. $12\text{-}15 \text{ m}^2 \text{ g}^{-1}$ (Kahle et al., 2002) and $8\text{-}19 \text{ m}^2 \text{ g}^{-1}$ (Punrattanasin and Sariem, 2015). Accounting for the BET surface area would decrease γ by a factor of 10^4 in our case.

3 Results and discussion

3.1 HCHO uptake reproducibility on soil

Chamber experiments have often been used to investigate the soil emission or uptake of trace gases. A common problem of chamber studies is that the results are not reproducible. Even for the same soil samples and experimental setup, the results may still differ from each other. This lack of reproducibility deteriorates the interpretation, extrapolation and application of experimental results.

The change of soil microbiological activities and soil micro-structure seems to be the two most probable reasons leading to non-reproducible results. If that's the case, sterilized soil with a well-defined structure/geometry can avoid these influences and present reproducible results. To test it, we performed three uptake experiments for the same soil sample under the same RH conditions. Before each experiment, the coated flow tube was flushed with pure N₂ (HCHO-free) until HCHO release ceased.

As shown in Fig. 3, almost identical uptake coefficients are determined from three experiments (each lasted for 50 minutes) at RH of 50% and HCHO concentration of ~35 ppbv. The reproducibility gives confidence in the kinetic parameter γ determined from the flow tube approach.

3.2 HCHO uptake on soil and temporal variation

Variation of uptake coefficients with time is a key question for evaluating the atmospheric relevance of surface uptake. Fast initial uptake can be unimportant if it quickly slows down due to consumption or occupation of reactive sites on surfaces (Kalberer et al., 1999). In this work, two 8-hour uptake experiments were performed to check the temporal variability of the HCHO uptake coefficients.

We first investigated the case under dry conditions (RH of ~0%), in which ~32 ppb of HCHO supplied by the HCHO generator was flushed through the flow tube. As shown in Fig. 4A, the largest HCHO uptake and decrease of HCHO concentration are found in the beginning of the uptake experiment. Within the 8-hour experiment, γ is reduced from $(1.1 \pm 0.05) \times 10^{-4}$ to $(5.5 \pm 0.4) \times 10^{-5}$. To extend the generality of such dependence, we also conducted the same experiment but at RH of 40%. As shown in Fig. 4B, the result reveals an even faster decay of γ over time suggesting an important role of water vapor in controlling the trace gas exchange at the atmosphere-soil interface.

3.3 Relative humidity (RH) effect

Water vapor has been suggested to influence the surface uptake for a variety of surface materials. On the one hand, it may compete for the reactive sites with other species and reduce their uptake (Ruiz et al., 1998; Goss et al., 2004; Donaldson et al.,

2014a). On the other hand, the condensed water may attract more water-soluble or hydrophilic molecules and enhance the uptake (Pei and Zhang, 2011). To better understand the role of water molecules, we examined the RH dependence of uptake coefficients. Each experiment lasted for 50 minutes with the same setup as the aforementioned 8-hour experiments.

5 Figure 5 shows the dependence of uptake coefficients of HCHO under different RHs. The highest value is achieved at dry conditions (RH of ~0%) and doesn't decrease much within the 50-minute experiment. Increasing RH results in a sharp decrease of γ , until reaching a RH threshold level of ~30%. Above 30% RH, γ becomes almost independent of RH. This RH effect could be expected for a longer uptake time period (e.g., 8 hours), as the uptake coefficients always show a large difference between dry and humid conditions during the 8-hour uptake experiments (Fig. 4A and Fig. 4B). For the detailed
10 mechanism of the RH influence on HCHO uptake, see Sect. 3.6.

3.4 Concentration effect

We also investigated the dependence of the uptake coefficients on initial HCHO concentrations, under dry and humid conditions (Fig. 6). Under dry conditions, higher HCHO concentrations (20 – 40 ppb) lead to significantly reduced uptake coefficients. The HCHO molecules themselves exert a competition for reactive sites. This effect almost ceases under
15 humidified conditions. As the number of water molecules is far more than that of HCHO and they both show competitive adsorption behavior on soil, it is conceivable that this concentration effect is weakened by increasing RH to 40%, further confirming the strong influence of water on the HCHO uptake.

Such a dependence on the initial concentrations of analytes under low RH conditions had already been reported by other
20 researchers. Sassine et al. (2010) investigated the HCHO uptake kinetics on TiO₂ mineral coatings and found that the inverse of the uptake rate depended linearly on the inverse of the HCHO inlet concentrations. Wang et al. (2012) measured the uptake of NO₂ onto soil using a coated-wall flow tube and also observed that uptake coefficients were negatively dependent on NO₂ gas phase concentrations. They both gave explanations based on the Langmuir-Hinshelwood mechanism, in which gas molecules compete for the adsorption sites and the adsorbed molecules undergo following reactions. At higher HCHO
25 concentrations (20 – 40 ppb) or/and higher water vapour partial pressure (RH = 40%), the soil surface becomes more easily covered by adsorbed HCHO or/and H₂O molecules that had not yet reacted, resulting in lower probability of successful collisions between HCHO and the soil surface and thus a lowering of the uptake coefficient.

3.5 Reversibility of HCHO uptake

The decay of initial uptake is a common feature for trace gas uptake on different surfaces. It can be explained by different
30 mechanisms, e.g., a process dominated by adsorption and chemical reactions; or a process governed by surface and bulk reactions. To explore the underlying mechanism, we conducted a back-flushing experiment and investigated the reversibility of HCHO uptake.

We first performed a standard experiment by flushing HCHO through a coated flow tube with RH of 50%. Then the same tube was flushed with pure N₂ (HCHO free) and the amount of HCHO released elucidated potential uptake reversibility. Figure 7 shows that indeed the HCHO adsorbed by soil can be released back to the gas phase. The areas enclosed by the uptake and emission curves (orange area S_a and yellow area S_e) represent the amount of HCHO adsorbed and re-emitted by the soil, respectively. S_a and S_e could be calculated by curve fitting and integration. As the emission curve doesn't end with infinitely approaching the zero air signal, a fitted curve is used to consider this infinite decrease of HCHO signal and infer the total amount of re-emitted HCHO, reflected by S_e . Two functions are tested for emission curve fitting (parameters as detailed in Table 1). These fitting functions are derived on the basis of HCHO mass conservation in the flow tube, that is, the increase in gas flow HCHO concentration equals the HCHO released from the soil due to desorption and/or oligomer dissociation at the same time. The mass decay rate of HCHO on the soil which is determined by HCHO mass M and the net rate coefficient k can be expressed as $dM/dt = -k \times M^n$ (k reflects the net effect of emission rate and dissociation reaction rate on the soil surface; n means the apparent order of reactions between HCHO molecules (e.g. oligomerization), if $n = 1$, no reactions between HCHO molecules). Note that the HCHO mass decay mentioned here only takes into account processes which could re-emit HCHO into the gas phase (reversible reactions) rather than those converting HCHO into other products (irreversible reactions), as the emission curve in Fig. 7 only represents the reversible fraction. By solving the above differential equation and further taking the derivative of $M(t)$, the HCHO concentration C in the gas flow can be identified as a function of time t , as shown in Table 1 ($C = f(x)$, $t = x$). Table 1 compares two fitting functions, with the first one only accounting for zero and first order reactions and the second one further involving second order reactions. The latter provides better fitting results, implying the existence of physical/chemical interactions between adsorbed HCHO molecules on the soil surface (e.g., hydration and oligomerization). Thus, the second fitting function is applied to infer the total amount of re-emitted HCHO. The re-emitted HCHO is $(70 \pm 15)\%$ ((average \pm one standard deviation)%) of that adsorbed in the uptake experiment (Fig. 7), while the residual $(30 \pm 15)\%$ remains in the soil. This partial reversibility suggests that HCHO uptake on soil is a combination of adsorption/desorption and chemical reactions.

To further explore the reasons for this partial reversibility, we conducted an energy dispersive X-ray (EDX) analysis of the soil sample. As shown in Fig. S.2, inorganic elements (mainly exist as minerals) dominate the soil composition and the low fraction of carbon is consistent with the measurement of soil organic matter (Sect. 2.1). Among the inorganic elements, silicon is most abundant followed by aluminium, calcium and iron, with their contents (wt%) being $\sim 64\%$, $\sim 13\%$, $\sim 6.3\%$ and $\sim 5.7\%$, respectively. The partial reversibility can be interpreted by the different uptake ability of various components. Carlos-Cuellar et al.(2003) reported that HCHO uptake was completely reversible on SiO₂ but only partly ($< 1\sim 15\%$) reversible on α -Al₂O₃ and α -Fe₂O₃. Xu et al. (2011) investigated the heterogeneous reactions of HCHO on the surface of γ -Al₂O₃ particles and concluded that the adsorbed HCHO was firstly oxidized to dioxymethylene and further to formate. The

fraction of silicon of ~70% (silicon content divided by the total amount of all inorganic elements) in the soil investigated here closely resembles the fraction of HCHO desorbed ((70 ± 15)%) from soil at zero air conditions.

Since mineral particles occupy the major volume (approximately 45% - 49%) of soils (DeGomez et al., 2015) and silicon minerals (e.g., silicon oxides) are fairly common in mineral particles, the partial reversibility of HCHO uptake as shown in Fig. 7 may be expected as a general feature for other similar types of soils.

3.6 Uptake mechanism

Pore diffusion and surface processes could both account for the uptake of HCHO by soils. For pore diffusion within soils, the time scale depends on the thickness of the soil layer and the specific diffusion coefficients. Morrissey et al. (1999) reported typical macroscopic diffusion coefficients of VOCs ranging from 10^{-2} to 10^{-4} $\text{cm}^2 \text{min}^{-1}$ for clay minerals. However, the effective diffusion coefficients of VOCs in soils depend on soil properties, e.g., soil porosity, pore geometry, grain size, soil water content etc. and on VOCs characteristics, e.g., molecular size, Henry's law constant, solubility etc. (Batterman et al., 1996). Adopting the above range and utilizing Fick's second law of diffusion for our experimental case, we estimate a time scale for HCHO diffusing through the soil layer from tens of seconds to several minutes. This time scale is much less than that for our uptake experiments (8 hours), indicating that pore diffusion is not the limiting factor of uptake. In this sense, the uptake of HCHO by soil could be described by a mechanism including both adsorption/desorption and reactions of adsorbed HCHO on the soil surface.

For the adsorption process (reaction 1), gas phase HCHO, HCHO(g), can react with a reactive site S on the soil surface and become adsorbed by soil. The adsorbed HCHO(ads) can desorb into gas phase and release the reactive site. Once adsorbed, individual HCHO molecules may react with adsorbed water (hydration) and/or further combine with other HCHO to form oligomers (Toda et al., 2014). On the other hand, HCHO(ads) can also be converted to other products through chemical reactions (reaction 2).



H₂O would also undergo adsorption/desorption processes (reaction 3), occupy the reactive site and compete with HCHO. The competing effect of water molecules depends on the number of water monolayers on the soil surface. Ong and Lion (1991a) classified such effect into three regimes in their study of trichloroethylene (TCE) sorption on soil minerals.

According to this mechanism, the first regime (regime I) is from dry conditions to one monolayer coverage of water on the soil surface, where direct soil-gas sorption is evident with strong competition between water and HCHO for adsorption sites on soil. The second regime (regime II) corresponds to one to five monolayers of water molecules, with likely interactions between HCHO and water including sorption of HCHO onto surface-bound water that may lead to hydration and further oligomerization of HCHO, and limited dissolution into these monolayers. The third regime (regime III) starts from approximately five layers of water molecules up to the water holding capacity of soil, where the sorption of HCHO is dominated by condensed water on soil with respective dependence on Henry's Law. In this regime, HCHO hydrates into methylene glycol or into polyoxymethylene glycols (oligomerization; Toda et al., 2014) which might further enhance the uptake of HCHO on soil.

10

Based on our BET experiment, one water monolayer forms at ~30% RH (Fig. 8) which is consistent with those values (20%-30%) reported by Donaldson et al. (2014a), Lammel (1999) and Goss (1993) retrieved across different soil types. For RH ≤ 30%, the HCHO sorption lies in the regime I, and water molecules show a large competing effect with HCHO as demonstrated by the strong negative dependence of γ on the RH (Fig. 5). For RH > 30%, the water effect moves to the regime II. In this regime the adsorbed water is highly structured and modified by interactions with the soil mineral surface (Goss, 1992), and the surface area available for gas sorption is also kept constant (Goss et al., 2004). The constant surface area could explain the relatively stable uptake coefficients of HCHO observed between 30% and 70% RH as shown in Fig. 5. We haven't reached regime III in our experiment (which would require a RH > 90%). According to Ong and Lion (1991a), the uptake in regime III follows Henry's law. So increasing RH will increase the solvent volume (or number of water molecules) on the soil surface and thus increase the adsorption capacity.

20

In addition to the interactions between HCHO and water molecules in different regimes mentioned above, the rates of adsorption/desorption versus the chemical reaction rates also come into play in the net exchange of HCHO.

During the uptake process, the rate expression for HCHO loss from the gas phase can be given by:

$$25 \quad -\frac{d[\text{HCHO}(\text{g})]}{dt} = k_a[\text{HCHO}(\text{g})][\text{S}] - k_d[\text{HCHO}(\text{ads})] \quad (4)$$

From the point of kinetic gas theory, this loss rate could also be described as:

$$-\frac{d[\text{HCHO}(\text{g})]}{dt} = \frac{\gamma_{\text{HCHO}} \omega_{\text{HCHO}}}{4} \times \frac{A_s}{V} \times [\text{HCHO}(\text{g})] = \frac{\gamma_{\text{HCHO}} \omega_{\text{HCHO}}}{2r} [\text{HCHO}(\text{g})] \quad (5)$$

where γ_{HCHO} is the uptake coefficient of HCHO, ω_{HCHO} is the thermal velocity of HCHO, A_s is the geometric surface area of the soil, V and r are the volume and radius of the flow tube, respectively. Equating Eq. (4) and Eq. (5) yields a positive correlation between $[\text{S}]$ and γ_{HCHO} . Increase of RH would decrease $[\text{S}]$ due to reaction 3 and thus further reduce the value of γ_{HCHO} . This further explains the RH dependence of γ as shown in Sect 3.3.

30

For the variation of adsorbed HCHO on soil surface during the uptake, the adsorption/desorption, oligomerization/dissociation and chemical reactions are all considered and the rate is given as:

$$\frac{d[\text{HCHO(ads)}]}{dt} = k_a[\text{HCHO(g)}][\text{S}] - k_d[\text{HCHO(ads)}] + (k_p - k_o)[\text{oligomers}] - k_r[\text{HCHO(ads)}] \quad (6)$$

5

At the start of uptake, [HCHO(ads)] is zero and only the forward reaction of adsorption is relevant. HCHO adsorbed onto the soil surface would accumulate and increase the rates of desorption, oligomerization and chemical reactions. [HCHO(ads)] will continuously grow until a steady state is established, in which case $d[\text{HCHO(ads)}]/dt = 0$ and the net loss of HCHO in the gas phase is dominated by chemical reactions on soil. Meanwhile, the oligomerization of adsorbed HCHO may serve as a temporary buffer, storing or releasing HCHO on soil. On the other hand, the emission of HCHO from soil can also be limited by dissociation of these oligomers and de-hydration of HCHO hydrates, this may explain the prolonged emission curve found in Fig. 7.

4 Conclusions

We investigated the HCHO uptake on soil surfaces by a coated-wall flow tube method. Soil exhibits strong capacity for absorbing gaseous HCHO, with initial γ ranging from $(1.4 \pm 0.08) \times 10^{-4}$ at 0% RH to $(3.0 \pm 0.3) \times 10^{-5}$ at 70% RH based on the geometric soil surface. Because of simultaneously acting adsorption/desorption processes, γ shows a strong temporal dependence with an initial peak and subsequent decay until a steady state is reached. We also find a clear RH dependence of γ , especially in the low RH range (e.g., $\leq 30\%$, under ambient pressure and temperature conditions) and little RH effect at RH $> 30\%$. The RH dependence of HCHO uptake can be explained by a transition of uptake pathways. Under low RH and water coverage (less than one monolayer) water molecules compete with gaseous HCHO for the adsorption sites on soil, while under high RH the soil surface is fully covered with water molecules providing a near constant amount of surface adsorption sites. Besides HCHO, a similar effect of RH had been reported for the soil uptake of other VOCs (Chiou and Shoup, 1985; Smith et al., 1990; Ong and Lion, 1991b, a; Pennell et al., 1992; Goss, 1993; Unger et al., 1996; Ruiz et al., 1998).

Our results also show that HCHO uptake on soil is a partially reversible process involving both adsorption/desorption and chemical reactions (see Fig. 9). The adsorption/desorption reveals a bi-directional exchange on soil surfaces in which soil could serve either as a source or as a sink depending on ambient conditions and trace gas concentrations. Because of the strong diurnal variability of ambient HCHO concentrations, soil water content, temperature and hence relative humidity, HCHO exchange at soil surfaces may quickly change its sign in a diurnal course as suggested for other trace gases such as HONO (Su et al., 2011; VandenBoer et al., 2015). The adsorption/desorption equilibrium and the competition effects of water vapour are likely to influence the atmosphere-soil exchange of other trace gases as well.

Acknowledgments

This study was supported by the Max Planck Society (MPG) and National Natural Science Foundation of China (41330635). Guo Li acknowledges the financial support from the China Scholarship Council (CSC). We are grateful to Sorowka Antje for her help with the SEM and EDX analysis of the soil sample.

5 Appendix A

Development and evaluation of the CKD-B method

The differential equation describing the analyte (HCHO for our experimental case) concentration C as a function of axial and radial position (z, r) in a flow tube, and a new boundary condition proposed in CKD are given as:

$$u \frac{\partial C}{\partial z} = D \frac{1}{r} \frac{\partial}{\partial r} \left(r \frac{\partial C}{\partial r} \right)$$

10 (7)

$$-D \frac{\partial C}{\partial r} \Big|_{\text{wall}} = C \frac{\bar{v}}{4} \frac{\gamma}{1 - \left(\frac{\gamma}{2}\right)}$$

(8)

$$-\frac{\partial C}{\partial r^*} \Big|_{r^*=1} = N_{Shw} C \quad \text{with} \quad r^* = \frac{r}{R} \quad (9)$$

15 in which u is the axial flow velocity and D is the gas diffusion coefficient under experimental conditions. \bar{v} is the mean molecular speed and γ is the uptake coefficient. N_{Shw} is the Sherwood number and R is the radius of the flow tube.

Equation (8) shows that C_{wall} (the concentration at the wall) is required to determine γ . However, the radial diffusion needs time and may result in a concentration gradient in the radial direction. Since we can only measure the averaged concentration instead of C_{wall} , the determination of γ cannot be achieved unless the C profile is determined first (Behnke et al., 1997; Monge et al., 2010; Sassine et al., 2010; Kebede et al., 2013) (for details see reference Murphy et al., 1987). Therefore the factor of $\gamma / (1 - \gamma / 2)$ rather than simply γ is used by Murphy et al. (1987) for a correction to the wall collision rate in the presence of a concentration gradient near the wall. Equation (9) is taken as a dimensionless form of Eq. (8).

For each given γ , a differential equation provided in CKD method (Eq. (7)) can be solved for a C profile and the functional relationship between transmittance of the analyte in the flow tube (C_{out}/C_{in} , C_{out} and C_{in} correspond to the concentrations of analyte at the outlet and the inlet of the flow tube, respectively) and γ (strictly the Sherwood number N_{Shw} as detailed in reference Murphy et al., 1987) can be established. Then by measuring the transmittance, we can determine the desired uptake

coefficients. It can be conceived that the γ - transmittance relation also depends on flow rate and the flow tube dimensions. Therefore, Murphy and Fahey (1987) provided a table of coefficients for a range of these parameters. When conditions were not available from the table, interpolation was often used in previous studies.

5 Here we directly solve the differential equation with numerical methods (code provided in the Supplement) rather than using interpolated values. As this operation is based on the CKD method, it can be specified as CKD-based method (CKD-B) and this nomenclature is adopted above. More recently, another new analytical method has been derived by Knopf, Pöschl and Shiraiwa (KPS), based on a recently developed kinetic flux model framework and models describing interactions of gas species with aerosol particles (Knopf et al., 2015) (for details see references therein). As the KPS method provides efficient
10 and robust analyses and predictions of gas and particle uptake in flow tube experiments encountering diffusion limitation, here, we make a comparison between CKD-B and KPS. Fig. S.3 shows that both methods agree very well for deriving the dependence of transmittance C_{out}/C_{in} on γ , under the specific flow rate and flow tube dimensions in our experimental case. To further test the accuracy of CKD-B method, the dependence of transmittance C_{out}/C_{in} on the Sherwood number (N_{Shw}) is compared between CKD-B and CKD as well. Fig. S.4 shows a good agreement between results from CKD (red dots) and
15 CKD-B (black line).

References

- Andreae, M. O., and Merlet, P.: Emission of trace gases and aerosols from biomass burning, *Global Biogeochem Cy*, 15, 955-966, 2001.
- Ayers, G. P., Gillett, R. W., Granek, H., deServes, C., and Cox, R. A.: Formaldehyde production in clean marine air, *Geophys Res Lett*, 24, 401-404, 1997.
- 20 Batterman, S., Padmanabham, I., and Milne, P.: Effective gas-phase diffusion coefficients in soils at varying water content measured using a one-flow sorbent based technique, *Environ Sci Technol*, 30, 770-778, 1996.
- Behnke, W., George, C., Scheer, V., and Zetzsch, C.: Production and decay of ClNO₂, from the reaction of gaseous N₂O₅ with NaCl solution: Bulk and aerosol experiments, *J Geophys Res-Atmos*, 102, 3795-3804, 1997.
- 25 Brunauer, S., Emmett, P. H., and Teller, E.: Adsorption of Gases in Multimolecular Layers, *J. Am. Chem. Soc.*, 60, 309-319, 10.1021/ja01269a023, 1938.
- Carlier, P., Hannachi, H., and Mouvier, G.: The Chemistry of Carbonyl-Compounds in the Atmosphere - a Review, *Atmos Environ*, 20, 2079-2099, 1986.
- Carlos-Cuellar, S., Li, P., Christensen, A. P., Krueger, B. J., Burrichter, C., and Grassian, V. H.: Heterogeneous uptake kinetics of volatile organic compounds on oxide surfaces using a Knudsen cell reactor: Adsorption of acetic acid, formaldehyde, and methanol on alpha-
30 Fe₂O₃, alpha-Al₂O₃, and SiO₂, *J Phys Chem A*, 107, 4250-4261, 2003.
- Chiou, C. T., and Shoup, T. D.: Soil Sorption of Organic Vapors and Effects of Humidity on Sorptive Mechanism and Capacity, *Environ Sci Technol*, 19, 1196-1200, 1985.
- Dasgupta, P. K., Dong, S., Hwang, H., Yang, H. C., and Genfa, Z.: Continuous Liquid-Phase Fluorometry Coupled to a Diffusion Scrubber for the Real-Time Determination of Atmospheric Formaldehyde, Hydrogen-Peroxide and Sulfur-Dioxide, *Atmos Environ*, 22,
35 949-963, 1988.
- DeGomez, T., Kolb, P., and Kleinman, S.: Basic Soil Components: <http://articles.extension.org/pages/54401/basic-soil-components>, 2015.
- DiGangi, J. P., Boyle, E. S., Karl, T., Harley, P., Turnipseed, A., Kim, S., Cantrell, C., Maudlin, R. L., Zheng, W., Flocke, F., Hall, S. R., Ullmann, K., Nakashima, Y., Paul, J. B., Wolfe, G. M., Desai, A. R., Kajii, Y., Guenther, A., and Keutsch, F. N.: First direct measurements of formaldehyde flux via eddy covariance: implications for missing in-canopy formaldehyde sources, *Atmos Chem Phys*,
40 11, 10565-10578, 2011.
- Donaldson, M. A., Berke, A. E., and Raff, J. D.: Uptake of Gas Phase Nitrous Acid onto Boundary Layer Soil Surfaces, *Environ Sci Technol*, 48, 375-383, 2014a.

- Donaldson, M. A., Bish, D. L., and Raff, J. D.: Soil surface acidity plays a determining role in the atmospheric-terrestrial exchange of nitrous acid, *Proceedings of the National Academy of Sciences*, 111, 18472-18477, 10.1073/pnas.1418545112, 2014b.
- Fried, A., McKeen, S., Sewell, S., Harder, J., Henry, B., Goldan, P., Kuster, W., Williams, E., Baumann, K., Shetter, R., and Cantrell, C.: Photochemistry of formaldehyde during the 1993 Tropospheric OH Photochemistry Experiment, *J Geophys Res-Atmos*, 102, 6283-6296, 1997.
- Fried, A., Crawford, J., Olson, J., Walega, J., Potter, W., Wert, B., Jordan, C., Anderson, B., Shetter, R., Lefer, B., Blake, D., Blake, N., Meinardi, S., Heikes, B., O'Sullivan, D., Snow, J., Fuelberg, H., Kiley, C. M., Sandholm, S., Tan, D., Sachse, G., Singh, H., Faloon, I., Harward, C. N., and Carmichael, G. R.: Airborne tunable diode laser measurements of formaldehyde during TRACE-P: Distributions and box model comparisons, *J Geophys Res-Atmos*, 108, 2003.
- Goss, K. U.: Effects of Temperature and Relative-Humidity on the Sorption of Organic Vapors on Quartz Sand, *Environ Sci Technol*, 26, 2287-2294, 1992.
- Goss, K. U.: Effects of Temperature and Relative-Humidity on the Sorption of Organic Vapors on Clay-Minerals, *Environ Sci Technol*, 27, 2127-2132, 1993.
- Goss, K. U., Buschmann, J., and Schwarzenbach, R. P.: Adsorption of organic vapors to air-dry soils: Model predictions and experimental validation, *Environ Sci Technol*, 38, 3667-3673, 2004.
- Gray, C. M., Monson, R. K., and Fierer, N.: Biotic and abiotic controls on biogenic volatile organic compound fluxes from a subalpine forest floor, *J Geophys Res-Biogeog*, 119, 547-556, 2014.
- Hak, C., Pundt, I., Trick, S., Kern, C., Platt, U., Dommen, J., Ordóñez, C., Prevot, A. S. H., Junkermann, W., Astorga-Llorens, C., Larsen, B. R., Mellqvist, J., Strandberg, A., Yu, Y., Galle, B., Kleffmann, J., Lorzer, J. C., Braathen, G. O., and Volkamer, R.: Intercomparison of four different in-situ techniques for ambient formaldehyde measurements in urban air, *Atmos Chem Phys*, 5, 2881-2900, 2005.
- Heikes, B., Lee, M. H., Jacob, D., Talbot, R., Bradshaw, J., Singh, H., Blake, D., Anderson, B., Fuelberg, H., and Thompson, A. M.: Ozone, hydroperoxides, oxides of nitrogen, and hydrocarbon budgets in the marine boundary layer over the South Atlantic, *J Geophys Res-Atmos*, 101, 24221-24234, 1996.
- Jacob, D. J., Heikes, B. G., Fan, S. M., Logan, J. A., Mauzerall, D. L., Bradshaw, J. D., Singh, H. B., Gregory, G. L., Talbot, R. W., Blake, D. R., and Sachse, G. W.: Origin of ozone and NO_x in the tropical troposphere: A photochemical analysis of aircraft observations over the South Atlantic basin, *J Geophys Res-Atmos*, 101, 24235-24250, 1996.
- Jacob, D. J.: Heterogeneous chemistry and tropospheric ozone, *Atmos Environ*, 34, 2131-2159, 2000.
- Jaegle, L., Jacob, D. J., Brune, W. H., Faloon, I., Tan, D., Heikes, B. G., Kondo, Y., Sachse, G. W., Anderson, B., Gregory, G. L., Singh, H. B., Poeschel, R., Ferry, G., Blake, D. R., and Shetter, R. E.: Photochemistry of HO_x in the upper troposphere at northern midlatitudes, *J Geophys Res-Atmos*, 105, 3877-3892, 2000.
- Junkermann, W., and Burger, J. M.: A new portable instrument for continuous measurement of formaldehyde in ambient air, *J Atmos Ocean Tech*, 23, 38-45, 2006.
- Kahle, M., Kleber, M., and Jahn, R.: Carbon storage in loess derived surface soils from Central Germany: Influence of mineral phase variables, *Journal of Plant Nutrition and Soil Science*, 165, 141-149, 2002.
- Kaiser, J., Li, X., Tillmann, R., Acir, I., Holland, F., Rohrer, F., Wegener, R., and Keutsch, F. N.: Intercomparison of Hantzsch and fiber-laser-induced-fluorescence formaldehyde measurements, *Atmos Meas Tech*, 7, 1571-1580, 2014.
- Kalberer, M., Ammann, M., Arens, F., Gaggeler, H. W., and Baltensperger, U.: Heterogeneous formation of nitrous acid (HONO) on soot aerosol particles, *J Geophys Res-Atmos*, 104, 13825-13832, 1999.
- Kebede, M. A., Varner, M. E., Scharko, N. K., Gerber, R. B., and Raff, J. D.: Photooxidation of Ammonia on TiO₂ as a Source of NO and NO₂ under Atmospheric Conditions, *Journal of the American Chemical Society*, 135, 8606-8615, 2013.
- Knopf, D. A., Poschl, U., and Shiraiwa, M.: Radial Diffusion and Penetration of Gas Molecules and Aerosol Particles through Laminar Flow Reactors, Denuders, and Sampling Tubes, *Anal Chem*, 87, 3746-3754, 2015.
- Kormann, R., Fischer, H., de Reus, M., Lawrence, M., Bruhl, C., von Kuhlmann, R., Holzinger, R., Williams, J., Lelieveld, J., Warneke, C., de Gouw, J., Heland, J., Ziereis, H., and Schlager, H.: Formaldehyde over the eastern Mediterranean during MINOS: Comparison of airborne in-situ measurements with 3D-model results, *Atmos Chem Phys*, 3, 851-861, 2003.
- Kulmala, M., and Petaja, T.: Soil Nitrites Influence Atmospheric Chemistry, *Science*, 333, 1586-1587, 2011.
- Lammel, G.: Formation of Nitrous Acid: Parameterisation and Comparison with Observations.286, 1999.
- Lee, Y. N., Zhou, X., Kleinman, L. I., Nunnermacker, L. J., Springston, S. R., Daum, P. H., Newman, L., Keigley, W. G., Holdren, M. W., Spicer, C. W., Young, V., Fu, B., Parrish, D. D., Holloway, J., Williams, J., Roberts, J. M., Ryerson, T. B., and Fehsenfeld, F. C.: Atmospheric chemistry and distribution of formaldehyde and several multioxygenated carbonyl compounds during the 1995 Nashville Middle Tennessee Ozone Study, *J Geophys Res-Atmos*, 103, 22449-22462, 1998.
- Li, X., Rohrer, F., Brauers, T., Hofzumahaus, A., Lu, K., Shao, M., Zhang, Y. H., and Wahner, A.: Modeling of HCHO and CHOCHO at a semi-rural site in southern China during the PRIDE-PRD2006 campaign, *Atmos Chem Phys*, 14, 12291-12305, 2014.
- Liu, S. C., Trainer, M., Carroll, M. A., Hubler, G., Montzka, D. D., Norton, R. B., Ridley, B. A., Walega, J. G., Atlas, E. L., Heikes, B. G., Huebert, B. J., and Warren, W.: A Study of the Photochemistry and Ozone Budget during the Mauna-Loa-Observatory Photochemistry Experiment, *J Geophys Res-Atmos*, 97, 10463-10471, 1992.

- Lowe, D. C., and Schmidt, U.: Formaldehyde (HCHO) measurements in the nonurban atmosphere., *Journal of Geophysical Research*, 88, 10844-10858, 1983.
- Monge, M. E., D'Anna, B., Mazri, L., Giroir-Fendler, A., Ammann, M., Donaldson, D. J., and George, C.: Light changes the atmospheric reactivity of soot, *Proceedings of the National Academy of Sciences of the United States of America*, 107, 6605-6609, 2010.
- 5 Morrissey, F. A., and Grismer, M. E.: Kinetics of volatile organic compound sorption/desorption on clay minerals, *J Contam Hydrol*, 36, 291-312, 1999.
- Murphy, D. M., and Fahey, D. W.: Mathematical Treatment of the Wall Loss of a Trace Species in Denuder and Catalytic-Converter Tubes, *Anal Chem*, 59, 2753-2759, 1987.
- Ong, S. K., and Lion, L. W.: Mechanisms for Trichloroethylene Vapor Sorption onto Soil Minerals, *J Environ Qual*, 20, 180-188, 1991a.
- 10 Ong, S. K., and Lion, L. W.: Effects of Soil Properties and Moisture on the Sorption of Trichloroethylene Vapor, *Water Res*, 25, 29-36, 1991b.
- Oswald, R., Behrendt, T., Ermel, M., Wu, D., Su, H., Cheng, Y., Breuninger, C., Moravek, A., Mougin, E., Delon, C., Loubet, B., Pommerening-Roser, A., Sorgel, M., Poschl, U., Hoffmann, T., Andreae, M. O., Meixner, F. X., and Trebs, I.: HONO Emissions from Soil Bacteria as a Major Source of Atmospheric Reactive Nitrogen, *Science*, 341, 1233-1235, 2013.
- 15 Parrish, D. D., Ryerson, T. B., Mellqvist, J., Johansson, J., Fried, A., Richter, D., Walega, J. G., Washenfelder, R. A., de Gouw, J. A., Peischl, J., Aikin, K. C., McKeen, S. A., Frost, G. J., Fehsenfeld, F. C., and Herndon, S. C.: Primary and secondary sources of formaldehyde in urban atmospheres: Houston Texas region, *Atmos Chem Phys*, 12, 3273-3288, 2012.
- Pei, J. J., and Zhang, J. S. S.: On the performance and mechanisms of formaldehyde removal by chemi-sorbents, *Chem Eng J*, 167, 59-66, 2011.
- 20 Pennell, K. D., Rhue, R. D., Rao, P. S. C., and Johnston, C. T.: Vapor-Phase Sorption of Para-Xylene and Water on Soils and Clay-Minerals, *Environ Sci Technol*, 26, 756-763, 1992.
- Preunkert, S., Legrand, M., Pepy, G., Gallee, H., Jones, A., and Jourdain, B.: The atmospheric HCHO budget at Dumont d'Urville (East Antarctica): Contribution of photochemical gas-phase production versus snow emissions, *J Geophys Res-Atmos*, 118, 13319-13337, 2013.
- Preunkert, S., Legrand, M., Frey, M. M., Kukui, A., Savarino, J., Gallee, H., King, M., Jourdain, B., Vicars, W., and Helmig, D.:
25 Formaldehyde (HCHO) in air, snow, and interstitial air at Concordia (East Antarctic Plateau) in summer, *Atmos Chem Phys*, 15, 6689-6705, 2015.
- Price, H., Jaegle, L., Rice, A., Quay, P., Novelli, P. C., and Gammon, R.: Global budget of molecular hydrogen and its deuterium content: Constraints from ground station, cruise, and aircraft observations, *J Geophys Res-Atmos*, 112, doi:10.1029/2006JD008152, 2007.
- Punrattanasin, P., and Sariem, P.: Adsorption of Copper, Zinc, and Nickel Using Loess as Adsorbents, *Pol. J. Environ. Stud.*, 24, 1259-1266, 10.15244/pjoes/30264, 2015.
- 30 Rodier, D. R., and Birks, J. W.: Evaluation of Isoprene Oxidation as an Interference in the Cartridge Sampling and Derivatization of Atmospheric Carbonyl-Compounds, *Environ Sci Technol*, 28, 2211-2215, 1994.
- Ruiz, J., Bilbao, R., and Murillo, M. B.: Adsorption of different VOC onto soil minerals from gas phase: Influence of mineral, type of VOC, and air humidity, *Environ Sci Technol*, 32, 1079-1084, 1998.
- 35 Sassine, M., Burel, L., D'Anna, B., and George, C.: Kinetics of the tropospheric formaldehyde loss onto mineral dust and urban surfaces, *Atmos Environ*, 44, 5468-5475, 2010.
- Seinfeld, J. H., and Pandis, S. N.: *Atmospheric Chemistry and Physics: From Air Pollution to Climate Change*, 2nd Edition, Wiley, New York, 2006.
- Smith, J. A., Chiou, C. T., Kammer, J. A., and Kile, D. E.: Effect of Soil Moisture on the Sorption of Trichloroethene Vapor to Vadose-Zone Soil at Pictinny Arsenal, New Jersey. , *Environ Sci Technol*, 24, 676-683, 1990.
- 40 Su, H., Cheng, Y. F., Oswald, R., Behrendt, T., Trebs, I., Meixner, F. X., Andreae, M. O., Cheng, P., Zhang, Y., and Poschl, U.: Soil Nitrite as a Source of Atmospheric HONO and OH Radicals, *Science*, 333, 1616-1618, 2011.
- Tie, X., Brasseur, G., Emmons, L., Horowitz, L., and Kinnison, D.: Effects of aerosols on tropospheric oxidants: A global model study, *J Geophys Res-Atmos*, 106, 22931-22964, 2001.
- 45 Toda, K., Yunoki, S., Yanaga, A., Takeuchi, M., Ohira, S. I., and Dasgupta, P. K.: Formaldehyde Content of Atmospheric Aerosol, *Environ Sci Technol*, 48, 6636-6643, 2014.
- Unger, D. R., Lam, T. T., Schaefer, C. E., and Kosson, D. S.: Predicting the effect of moisture on vapor-phase sorption of volatile organic compounds to soils, *Environ Sci Technol*, 30, 1081-1091, 1996.
- Usher, C. R., Michel, A. E., and Grassian, V. H.: Reactions on mineral dust, *Chem Rev*, 103, 4883-4939, 2003.
- 50 VandenBoer, T. C., Young, C. J., Talukdar, R. K., Markovic, M. Z., Brown, S. S., Roberts, J. M., and Murphy, J. G.: Nocturnal loss and daytime source of nitrous acid through reactive uptake and displacement, *Nature Geoscience*, 8, 55-60, 10.1038/ngeo2298, 2015.
- Wagner, V., von Glasow, R., Fischer, H., and Crutzen, P. J.: Are CH₂O measurements in the marine boundary layer suitable for testing the current understanding of CH₄ photooxidation?: A model study, *J Geophys Res-Atmos*, 107, 2002.
- Wang, L., Wang, W. G., and Ge, M. F.: Heterogeneous uptake of NO₂ on soils under variable temperature and relative humidity conditions, *J Environ Sci-China*, 24, 1759-1766, 10.1016/S1001-0742(11)61015-2, 2012.
- 55

Weller, R., Schrems, O., Boddenberg, A., Gab, S., and Gautrois, M.: Meridional distribution of hydroperoxides and formaldehyde in the marine boundary layer of the Atlantic (48 degrees N-35 degrees S) measured during the Albatross campaign, *J Geophys Res-Atmos*, 105, 14401-14412, 2000.

5 Xu, B. Y., Shang, J., Zhu, T., and Tang, X. Y.: Heterogeneous reaction of formaldehyde on the surface of gamma-Al₂O₃ particles, *Atmos Environ*, 45, 3569-3575, 2011.

Zhou, X. L., Lee, Y. N., Newman, L., Chen, X. H., and Mopper, K.: Tropospheric formaldehyde concentration at the Mauna Loa observatory during the Mauna Loa observatory photochemistry experiment 2, *J Geophys Res-Atmos*, 101, 14711-14719, 1996.

10 List of Tables:

Table 1. Parameters of fitting functions.

| Functions | Coefficients (with 95% confidence bounds) | | | | | Goodness of fit R^2 |
|--|--|------------------------|-------------------------|-------------------------|-------------------------|-----------------------------|
| | a | b | c | d | e | |
| $f(x) =$ $a + b \times \exp(-c \times x)$ | -1.18×10^{-8} | 39.7 (38.35, 41.04) | 0.616 (0.607, 0.625) | | | 0.944 |
| $f(x) =$ $a + b \times \exp(-c \times x) + d \times (e - d \times x)^2$ | -1.15×10^{-4} (-0.456, 0.455) | 3.13 (2.35, 3.91) | 0.214 (0.094, 0.333) | 0.140 (0.121, 0.160) | 0.264 (0.221, 0.308) | 0.998 |

15

20

Figure Captions:

Figure 1. Characteristic morphology of coated soil layer observed by means of SEM (scanning electron microscope). (A) Flow tube cross-section view: the red arrow indicates the thickness of the soil layer and the blue arrow denotes the thickness of the glass tube. (B) View of the soil surface structure from above.

Figure 2. Schematic of the experimental setup. For details see text.

Figure 3. Effect of repeated uptake and emission on soil uptake coefficients within the uptake time range of 50 min at 50% RH.

10

Figure 4. Observed HCHO (green diamonds) at the flow tube outlet and uptake coefficients (orange circles) as (A) ~32 ppb of HCHO is exposed to soil at 0% RH and (B) ~35 ppb of HCHO is exposed to soil at 40% RH. The bars with different colors indicate the time periods corresponding to different gas supply: purple bars (N_2), blue bar (N_2 after flowing through the soil-coated tube), pink bars (generated HCHO), green bar (HCHO after flowing through reference tube), orange bar (HCHO after flowing through soil-coated tube).

15

Figure 5. Uptake coefficients variation as a function of uptake time, under different RHs. The error bars represent the standard deviation of three replicate experiments.

Figure 6. Dependence of uptake coefficients on initial HCHO concentrations at 0% and 40% RH, after uptake time periods of 5 min (red), 10 min (green), 20 min (orange), 30 min (blue) and 40 min (purple) (A); and uptake coefficients as a function of uptake time period at 0% RH (B); both under ambient pressure and 296 K. The error bars represent the standard deviation of three replicate experiments.

20

Figure 7. Reversible uptake of HCHO onto soil at 50% RH. The yellow bar represents the time period when flushing with N_2 just after the uptake experiment; other color bars as in Fig. 4.

25

Figure 8. Number of soil surface water monolayers, based on gravimetric analysis of water uptake and soil surface area determined by the BET method.

Figure 9. Schematic of HCHO uptake by soil surfaces.

30

List of Figures:

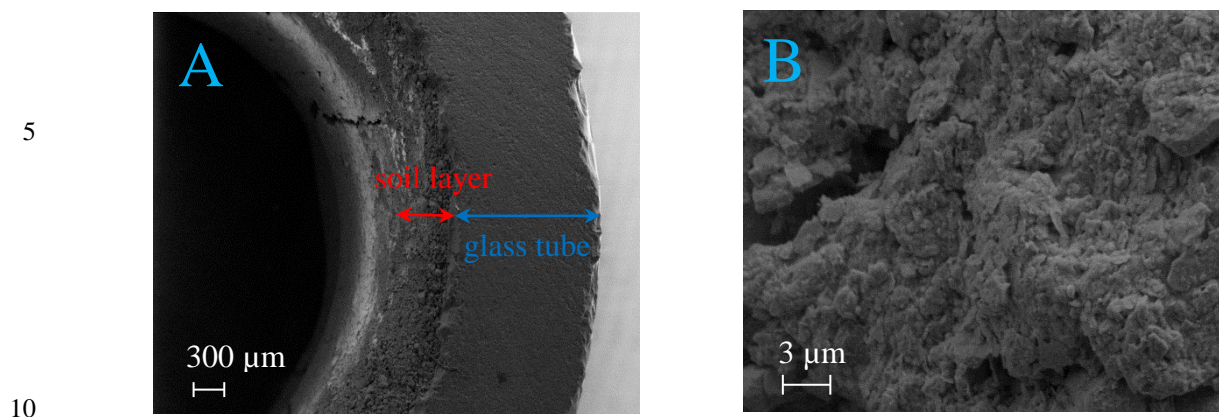


Figure 1.

15

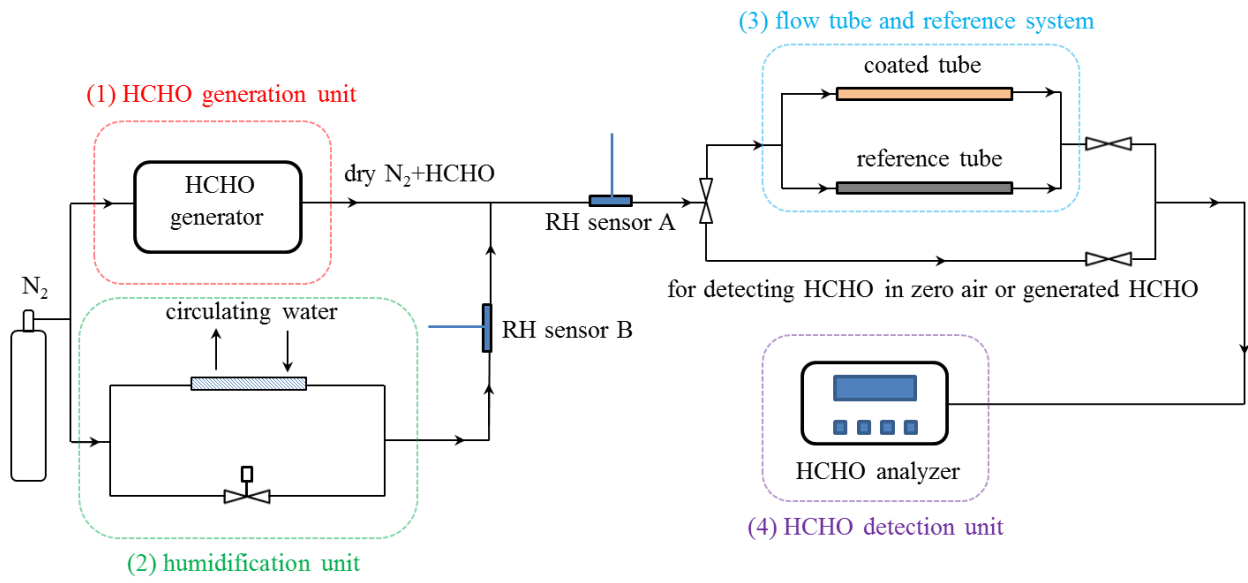


Figure 2.

5

10

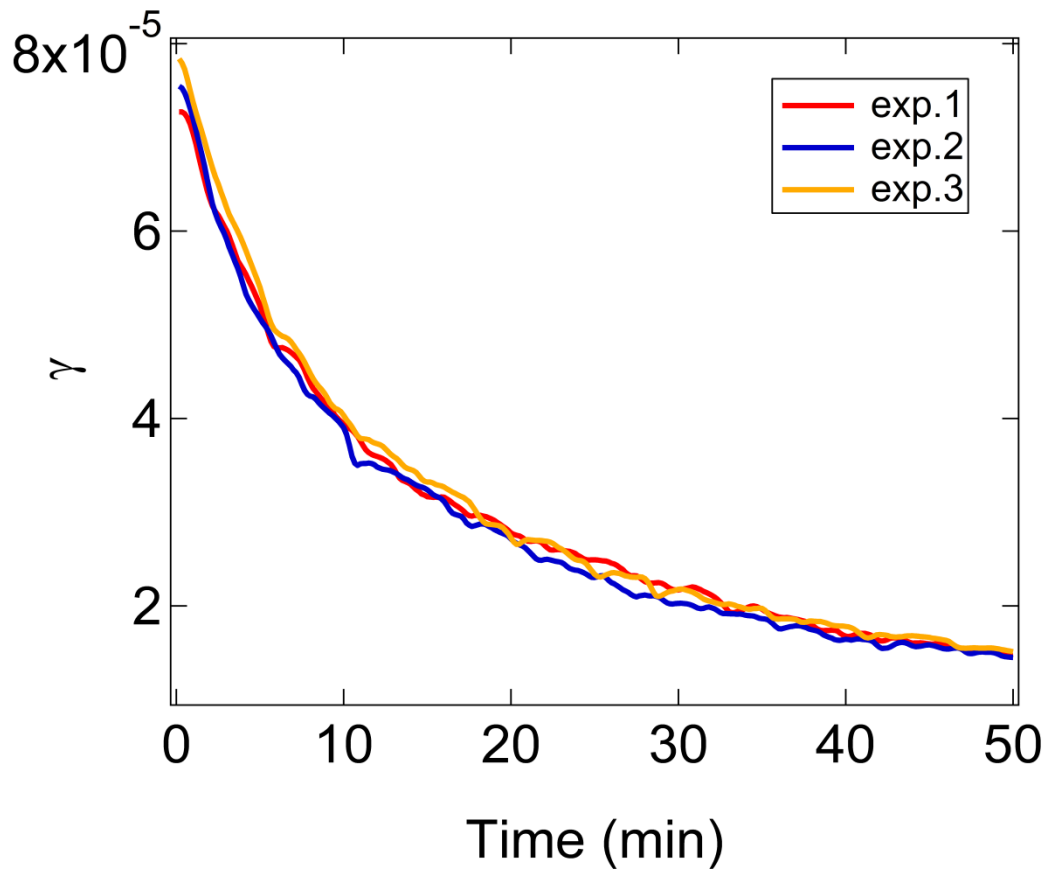


Figure 3.

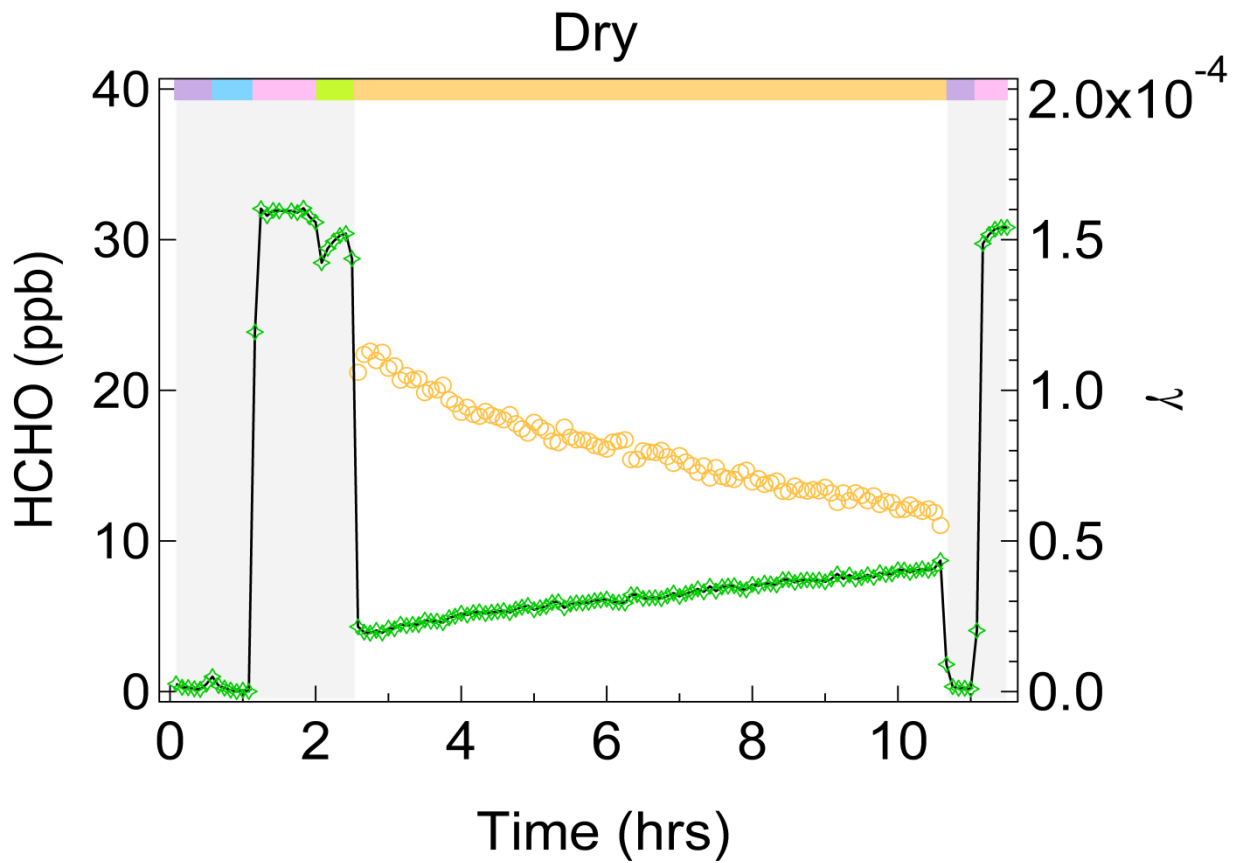


Figure 4. (A)

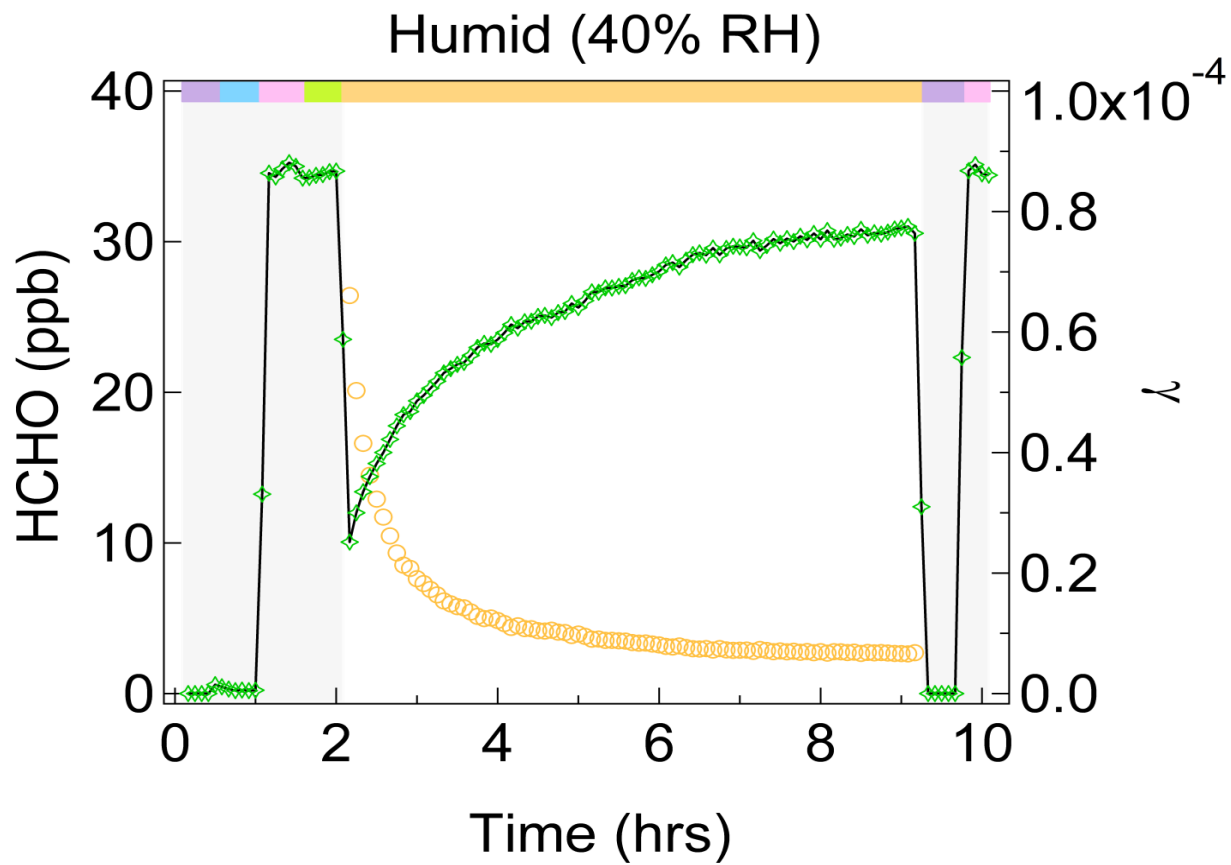


Figure 4. (B)

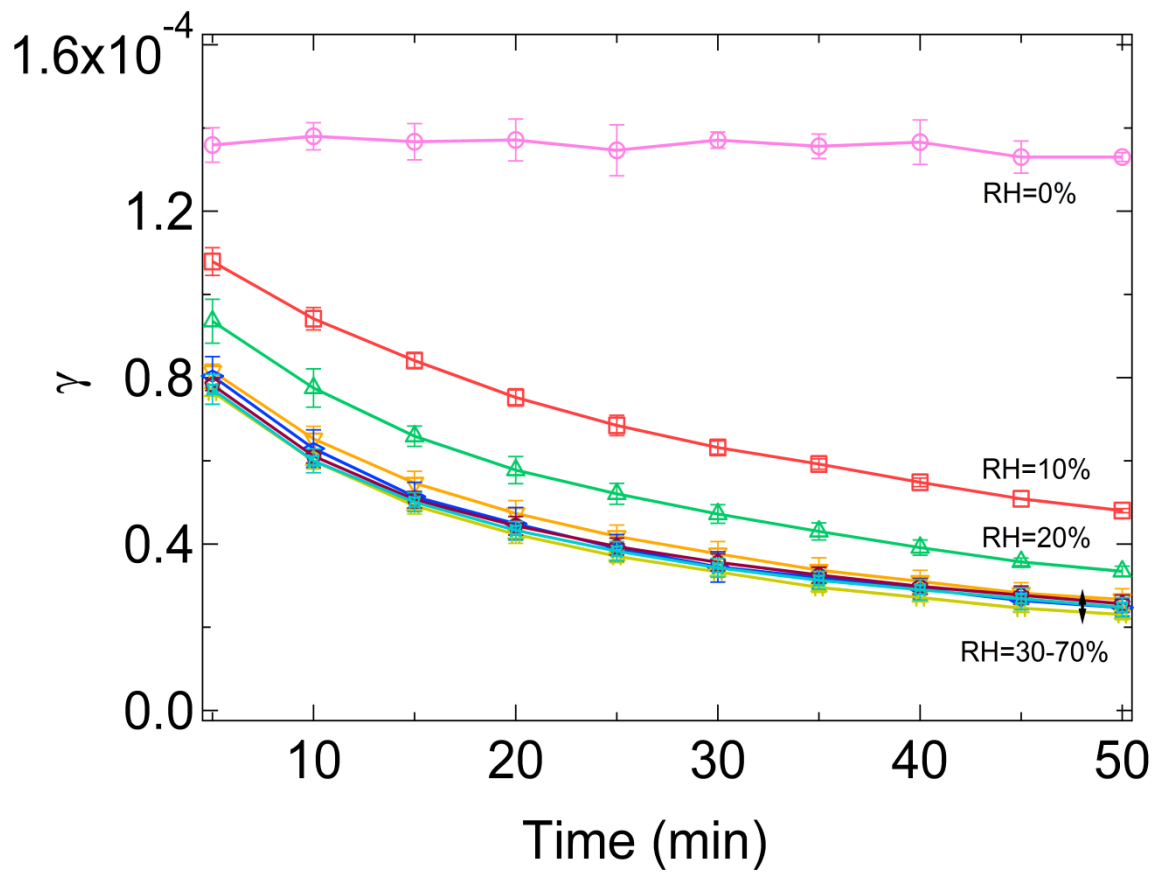


Figure 5.

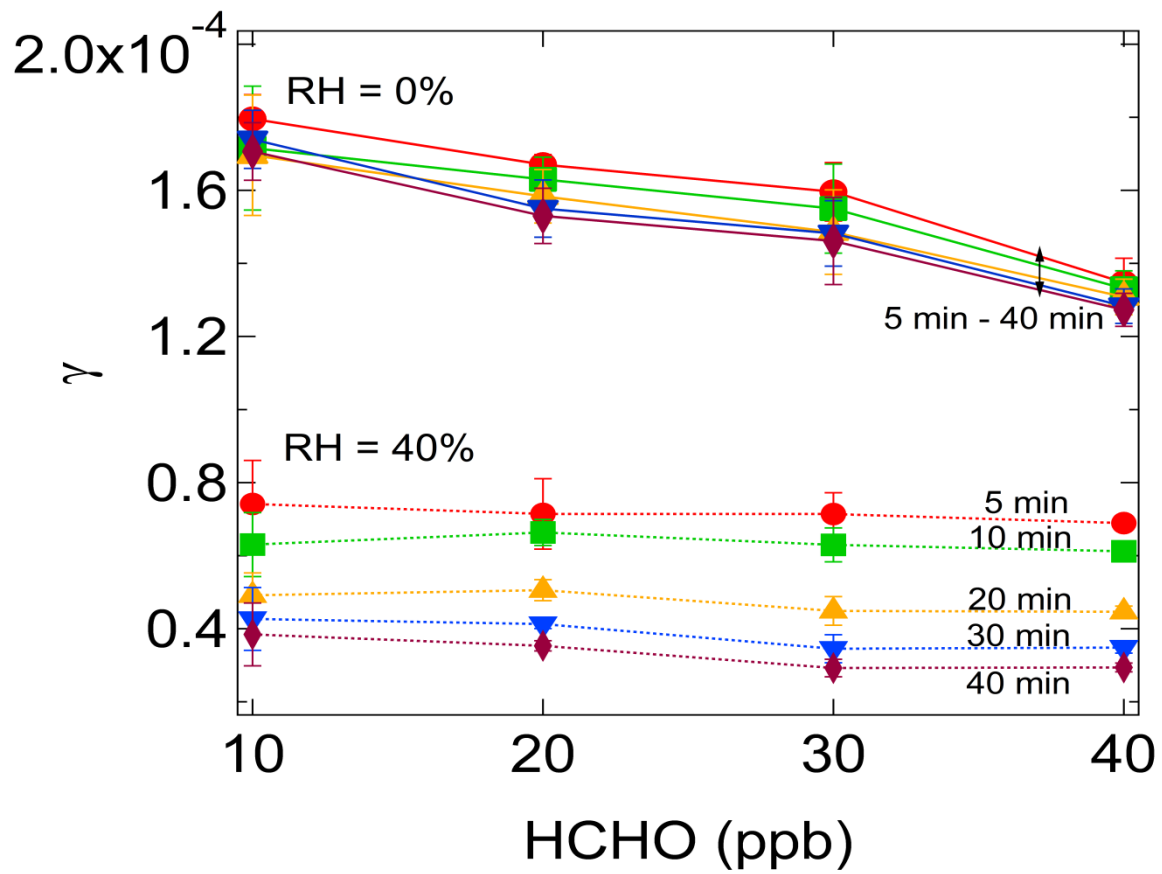


Figure 6. (A)

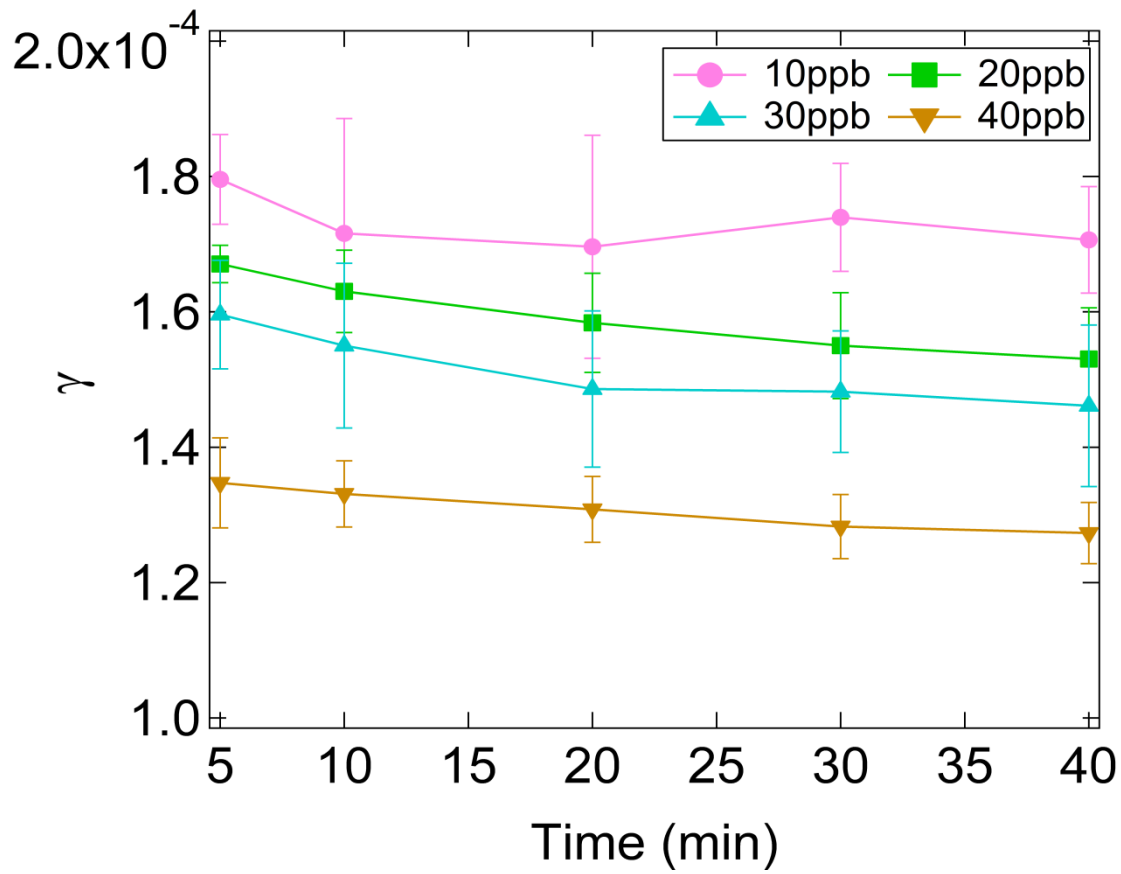


Figure 6. (B)

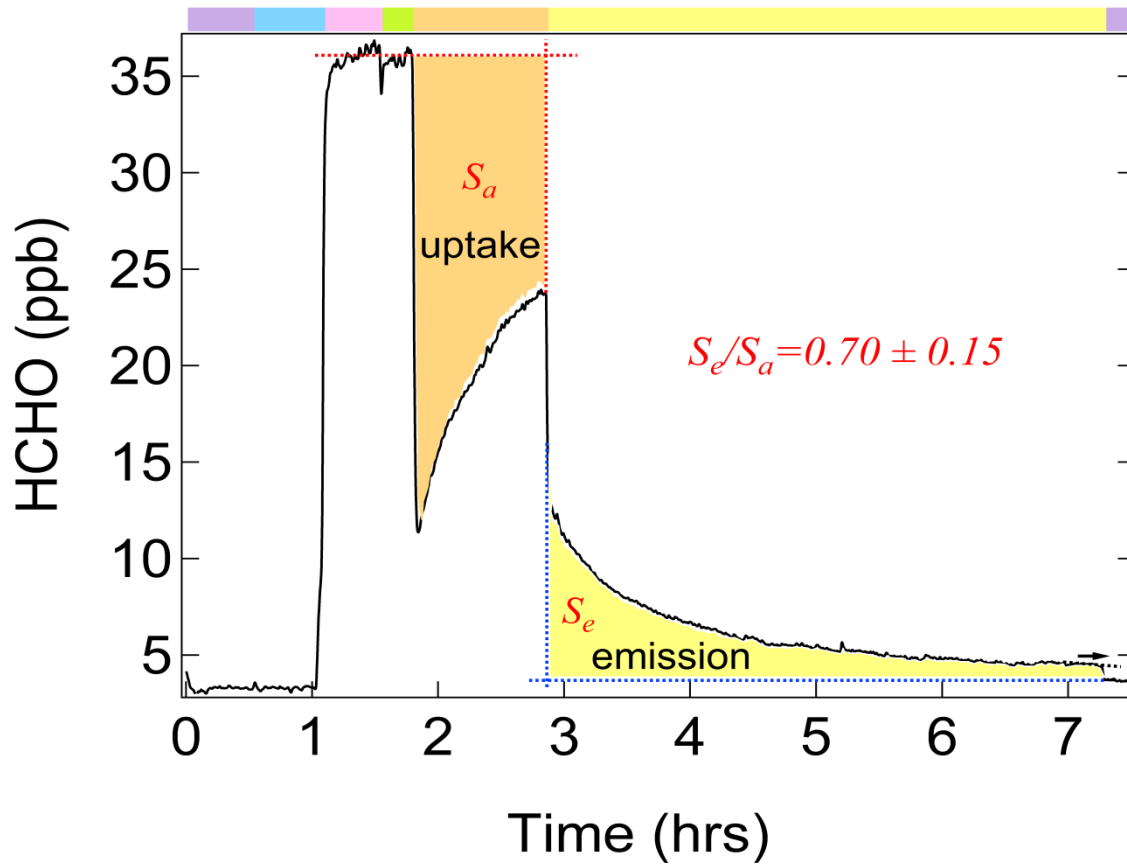


Figure 7.

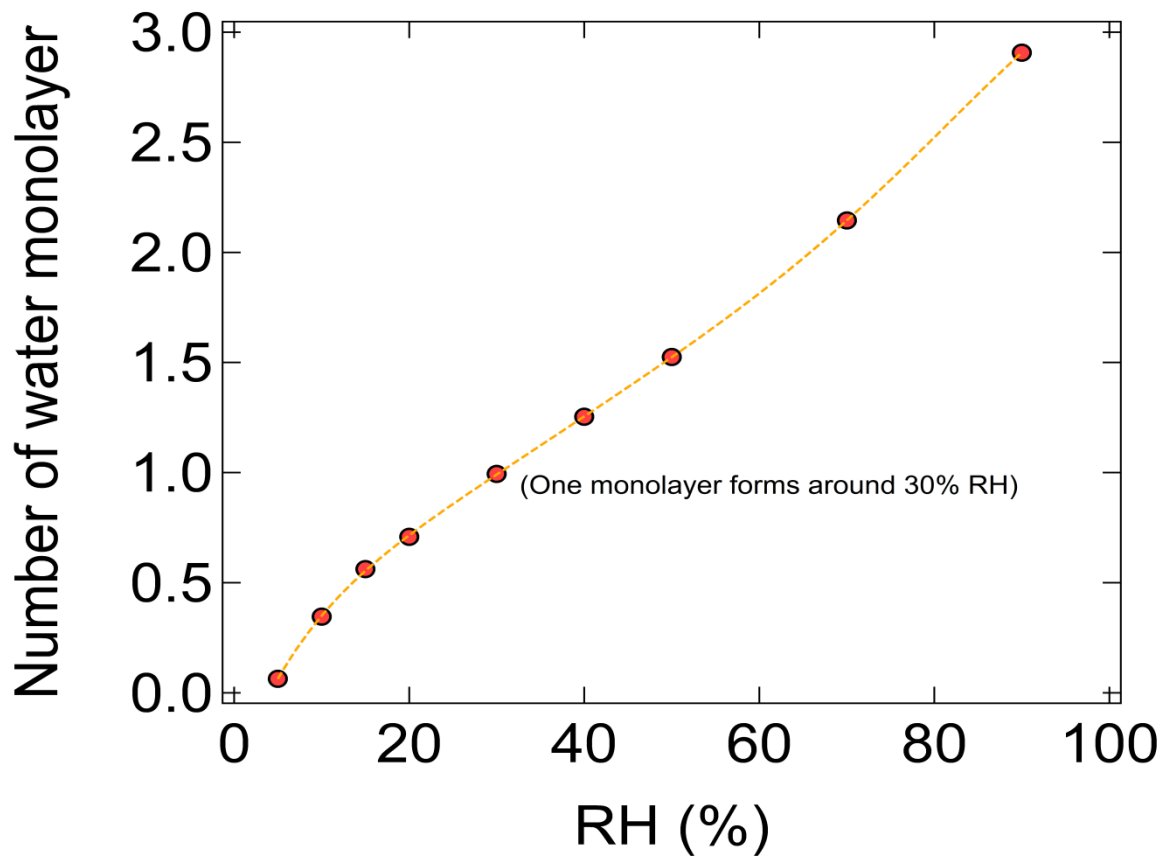


Figure 8.

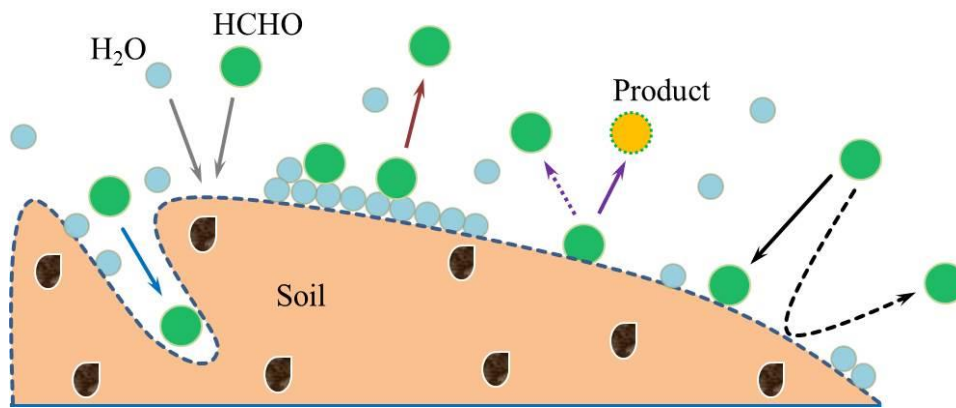


Figure 9.

5

10

15